

Thermal modelling of the human eye exposed to infrared radiation of 1064 nm Nd:YAG and 2090 nm Ho:YAG lasers

M. Cvetković¹, A. Peratta² & D. Poljak¹

¹*University of Split, Faculty of Electrical Engineering, Mechanical Engineering and Naval Architecture, Croatia*

²*Wessex Institute of Technology, UK*

Abstract

In the last few decades laser eye surgery has been implemented in various ophthalmic procedures. The most important issue with laser eye surgery is the estimation of temperature rise in eye tissues due to the absorption of high intensity laser radiation. The 2D model of the human eye, using the Finite Elements Method, is developed in order to study the temperature distribution in human eyes subjected to radiation by two infrared lasers, the 1064 nm Nd:YAG and the 2090 nm Ho:YAG laser. The mathematical model is based on the space–time dependent Pennes' bio-heat transfer equation supplemented with natural boundary condition equations for the cornea and the sclera. The results could prove to be useful in predicting the damage to intraocular tissues due to heating by infrared laser radiation.

1 Introduction

Among many possible applications for lasers, medical laser surgery represents definitely the most significant advance. In the last few decades laser eye surgery has become implemented in ophthalmology using a variety of laser systems.

From the increasing number of laser uses and the spread of different types of eye surgery, the need for quantitative understanding of basic laser–tissue interaction has arisen. Due to this fact, a number of models were developed to predict the various processes inside the human eye, with the ultimate goal of helping medical doctors in minimizing the possible damage to intraocular tissue while operating with lasers.



Light interacts with tissue in four different ways: transmission, reflection, scattering, and absorption. Among these, absorption is perhaps the most important process in modelling this interaction, since absorbed photon energy by tissue could be reemitted as radiant energy or transformed into heat.

Blood flow is a key element in thermoregulation of the living organism. Human eye is a special case, since the blood flow cannot regulate the heating inside the ocular tissue, so, thermal model of human eye is required.

In order to derive a model which describes laser thermal effects, heat transfer need to be taken into account. In biological tissues, this is achieved by using the Pennes' bioheat transfer equation, which takes into account different types of transfer processes.

Aim of this model is to provide the results for temperature distribution evolution inside the human eye, exposed to two infrared laser wavelengths, 1064 nm Nd:YAG and 2090 nm Ho:YAG, widely used in ophthalmology operations, such as posterior capsulotomy (after-cataract), peripheral iridotomy (treatment of glaucoma), for retinal photocoagulation (Nd:YAG) and for contactless thermal keratoplasty (Ho:YAG) [1, 2].

2 The mathematical statement

2.1 Historical background

Few of the first attempts to quantify the effects of electromagnetic radiation on temperature rise inside the eye were made by Taflove and Brodwin [3], and Emery et al. [4], who computed the intraocular temperatures in the eye due to microwave radiation using the finite difference and finite elements methods, respectively. Later, Scott [5, 6] developed a 2D FEM model of heat transfer in human eye to study the cataract formation due to infrared radiation. Also, Lagendijk [7] used the finite difference method to calculate the temperature distribution in human and animal eyes during hyperthermia treatment.

Regarding the laser–tissue thermal interaction, Mainster made one of the earliest analysis of the thermal response of clear ocular media to infrared laser radiation [8], and Amara [9] developed a thermal model of the human eye exposed to laser radiation using the finite elements. Sbirlea and L'Huillier [10] modelled the human eye exposed to argon laser using the 3D FEM, and Chua et al. [11] studied the temperature distribution within the human eye subjected to a laser source.

In recent years, authors use even more powerful numerical methods to solve heat transfer problems in human eye. Dodig [12] used hybrid FEM/BEM to investigate the influence of high frequency time harmonic EM fields on the human eye and Peratta [13] modelled the human eye exposed to conductive keratoplasty procedure, using the 3D boundary element method.



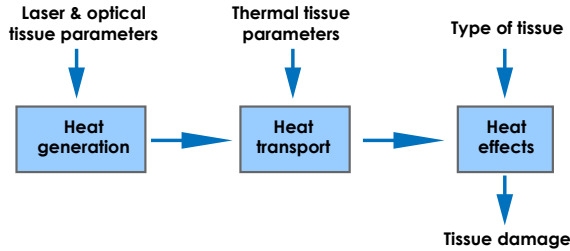


Figure 1: Parameters required for modelling thermal interaction.

Table 1: Thermal and optical properties of various human eye tissues.

Tissue type	Volumetric perfusion rate W_b	Internal volumetric heat generation Q_m	Thermal conductivity k	Specific heat capacity C	Abs.coef. (1064nm)	Abs.coef. (2090nm)
Vitreous humour	0	0	0.594	3997	20	542.7
Lens	0	0	0.400	3000	43.5	2558
Aqueous humour	0	0	0.578	3997	35	2228
Cornea	0	0	0.580	4178	113	2923
Sclera	0	0	0.580	4178	634.8	2923
Ciliary body	2700	690	0.498	3340	42.5	2228
Choroid	0	0	0.530	3840	6615	6398
Retina	35000	10000	0.565	3680	10000	4370

2.2 Human eye modelling

Although relatively small organ in the human body, the eye is a very complex optical system. This ovoid organ measures about 24 mm in length and 23 mm in diameter. We have assumed eye to be a solid structure of given dimensions, consisting of total of eight homogeneous tissues, namely, cornea, aqueous humour, ciliary body, lens, vitreous humour, retina, choroid and sclera.

The spatial extent and degree of tissue damage depends primarily on laser parameters such as wavelength, power density, exposure time, spot size, and repetition rate, but also on optical tissue properties like absorption and scattering coefficients, and thermal tissue properties such as heat capacity and thermal conductivity needs to be taken into account.

Figure 1 shows flow chart with important parameters required for modelling thermal interaction such is the laser-eye case.

Heat generation inside tissue is determined by laser parameters and optical tissue properties, but even when no external sources are present, important parameters such as volumetric perfusion rate of blood W_b and the internal volumetric heat generation Q_m , i.e. metabolic rate, need to be taken into account. They are always present in the organism, and are responsible for the constant temperature of body.

On the other hand, the transport of heat to the surrounding tissues is solely characterized by the tissue thermal conductivity k and specific heat capacity C . Data on these tissue parameters are given in Table 1, taken primarily from [14].

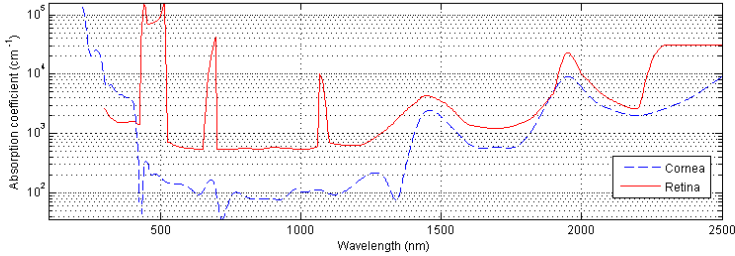


Figure 2: Absorption coefficient for cornea and retina.

Most important among optical tissue properties is the coefficient of absorption. In biological tissues, absorption is mainly due to the presence of water molecules, proteins, pigments, and other macromolecules, and is governed by Lambert–Beer’s law. The absorption coefficient strongly depends on the wavelength of the incident laser radiation as seen from Fig. 2. In the infrared region of the spectrum, it can be primarily attributed to water molecules, while proteins and pigments are main absorbers in the UV and visible range of the spectrum [15–17].

Values for absorption coefficient of various eye tissue are given in Table 1, taken from [18].

2.3 Bioheat transfer equation

The mathematical model of the human eye is based on the Pennes’ bioheat transfer equation [19], since it still is the foundation for all mathematical analysis in the field of bioheat transfer [20]. In Pennes’ model, the rate of tissue temperature increase is given by the sum of the net heat conduction into the tissue, metabolic heat generation, and the heating (cooling) effects due to arterial blood flow:

$$\rho C \frac{\partial T}{\partial t} = \nabla (k \nabla T) + W_b C_{pb} (T_a - T) + Q_m + H \tag{1}$$

Bioheat equation is extended with the new term H representing heat generated inside the tissue due to some external source. In our case, this source is laser radiation, but it could be any other source of electromagnetic radiation.

This equation is supplemented with natural boundary condition equations for cornea, sclera and domain inside the eye, respectively:

$$-k \frac{\partial T}{\partial n} = h_c (T - T_{amb}) + \sigma \epsilon (T^4 - T_{amb}^4) \in \Gamma_1 \tag{2}$$

$$-k \frac{\partial T}{\partial n} = h_s (T - T_a) \in \Gamma_2 \tag{3}$$

$$-k \frac{\partial T}{\partial n} = 0 \in \Gamma_3 \quad (4)$$

where k is specific tissue thermal conductivity given in Table 1, h_c heat transfer coefficient of cornea, h_s heat transfer coefficient of sclera, σ Stefan–Boltzmann constant, ϵ emissivity of the corneal surface, T_{amb} temperature of the ambient air anterior to the cornea, and T_a arterial blood temperature taken to be 36.7°C. The value for h_c is taken to be 14 W/m²°C, h_s is 65 W/m²°C, emissivity of the cornea is 0.975, and the value of ambient temperature is 30°C.

Equations (2) and (3) describe the thermal exchange between cornea and surrounding air due to convection and radiation, and thermal exchange between sclera and ocular globe due to convection only, respectively. Second term on the right hand-side of Eq. (2) is approximated by $\sigma \epsilon T_F^3 (T - T_{amb})$, where T_F is the melting temperature of the substance [9]. The value for T_F is taken to be 100°C.

2.4 Laser source modelling

Energy density $H(r, z, t)$, absorbed by the eye tissue at the n^{th} node with cylindrical coordinates (r, z) , is given by a product

$$H(r, z, t) = \alpha I(r, z, t) \quad (5)$$

where α is the wavelength dependent absorption coefficient of the specific tissue, given in Table 1, and I is the irradiance of the n^{th} node, given by

$$I(r, z, t) = I_0 \exp\left(-\frac{2r^2}{w^2} - \alpha z\right) \exp\left(-\frac{8t^2}{\tau^2}\right) \quad (6)$$

where I_0 is the incident value of intensity, w is the beam waist, and τ is the pulse duration.

For a given laser parameters, the irradiance at the cornea is calculated from $I_c = 4P/d_c^2\pi$, where P is laser power and d_c is a beam diameter on the cornea. Taking into account the focusing action of the lens, diameter of the image and irradiance on the retina is calculated from

$$d_r = 2.44 \frac{\lambda f}{d_p} \quad (7)$$

and

$$I_r = I_c \frac{d_p^2}{d_r^2} \quad (8)$$

where λ is laser wavelength, f focal distance of the lens, and d_p diameter of pupil opening. From these values, we now interpolate the intermediate values for the beam width, irradiance and energy density along the beam path.

The parameters for Nd:YAG laser, used in model are; pulse duration 1 ms, laser power 0.16 W, beam diameter on the cornea 8 mm, and pupil diameter 8.9 mm.



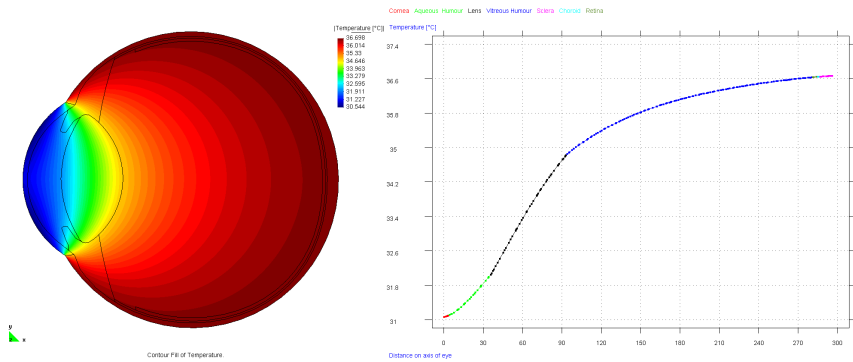


Figure 3: Steady-state case distribution of the temperature in the human eye and temperature along the eye pupillary axis. Length from anterior of cornea to posterior of sclera equals 24 mm.

Laser pulse was sampled in ten 0.1 ms steps, and in each of these steps, calculation of temperature distribution has been done. Following the laser cut-off, for the next five steps (2 s each), tissue cooling was simulated. Parameters for Ho:YAG laser are taken from [69], and they are: pulse duration 1 ms, energy density 31 J/m^2 , and beam diameter on the cornea 1.8 mm.

2.5 Numerical method

Analytical solution of the bioheat equation is limited to a few simple geometries with high degree of symmetry, but using the Finite Elements Method we are able to solve problems on complex geometries such as human eye.

The equation (1) is discretized in two spatial dimensions and solved using the weak formulation and the Galerkin–Bubnov procedure. A total number of 21,595 triangular elements and 11,094 nodes were generated using the GID 7.2 mesh generator. Solving part was done by algorithm written in MATLAB.

First, the equation is solved for the steady-state case, i.e. when no external sources are present. Latter, these results are used as initial conditions in the time domain analysis with included external source, i.e. laser radiation.

3 Results

3.1 Steady-state case

The results for the steady-state case temperature distribution in the human eye and temperature along the pupillary axis are shown in Fig. 3.

Steady–state case results, used latter as initial condition for time–domain analysis, are in a good agreement with number of papers [5, 9, 11, 21, 22]. One can note in Fig. 3 a steady rise of temperature from anterior to posterior parts of the eye,

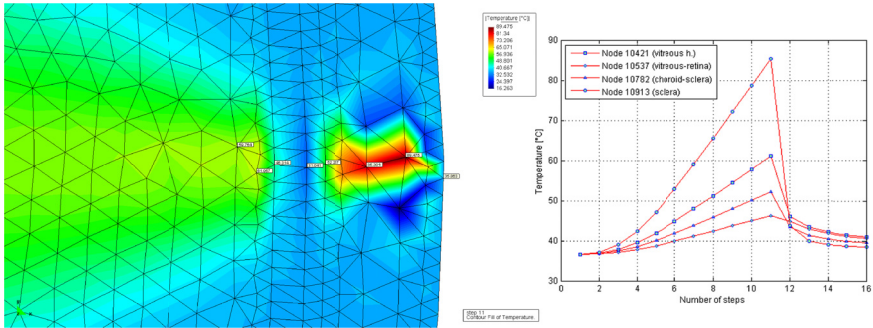


Figure 4: Detail of temperature distribution around posterior part of the eye, and temperature evolution of nodes in vitreous, vitreo-retinal boundary, chorio-scleral boundary and sclera for 1 ms exposure and relaxation after source cancelling, achieved with 1064 nm Nd:YAG laser.

with steepest slope being within lens tissue. Reason for this is lowest value for thermal conductivity of lens, compared to other eye tissues.

3.2 Time domain analysis

3.2.1 1064 nm Nd:YAG laser

Maximum temperature of 89.475°C, for Nd:YAG laser, is obtained on a node on sclera, as shown on Fig. 4, detailing the temperature distribution around posterior part of the eye. Same figure on the right shows also the temperature evolution on selected nodes. Amara [9] reported maximum temperature increase of 74°C, independent of laser exposure time, while we believe that exposure time is very important parameter, and significantly influence the temperature rise in human eye.

On Figure 5, evolution for the whole eye temperature distribution can be seen, with same laser setup. Animation files could be obtained from [23].

3.2.2 2090 nm Ho:YAG laser

Calculation for the 2090 nm Ho:YAG laser radiation yielded the maximum temperature of 69.424°C on cornea–aqueous boundary, after 1 ms exposure, as shown on Fig. 6. Few seconds after the cancellation of laser source, temperature distribution in the eye equals that of steady–state case, shown on the left, on same Figure. Podol'tsev [2] reported maximum rise of 19.8°C at the center of laser spot, for this wavelength.

We can also note, that for this laser wavelength, while temperature of the vitreous humour posterior to lens rises to approximately 40°C, temperature distribution through the lens is same as for steady–state case.

It has been known that lens functions as an optical filter for UV radiation, but we can see that even for infrared radiation it plays significant role. This could be explained mainly by the high absorption coefficient of the lens in those ranges of

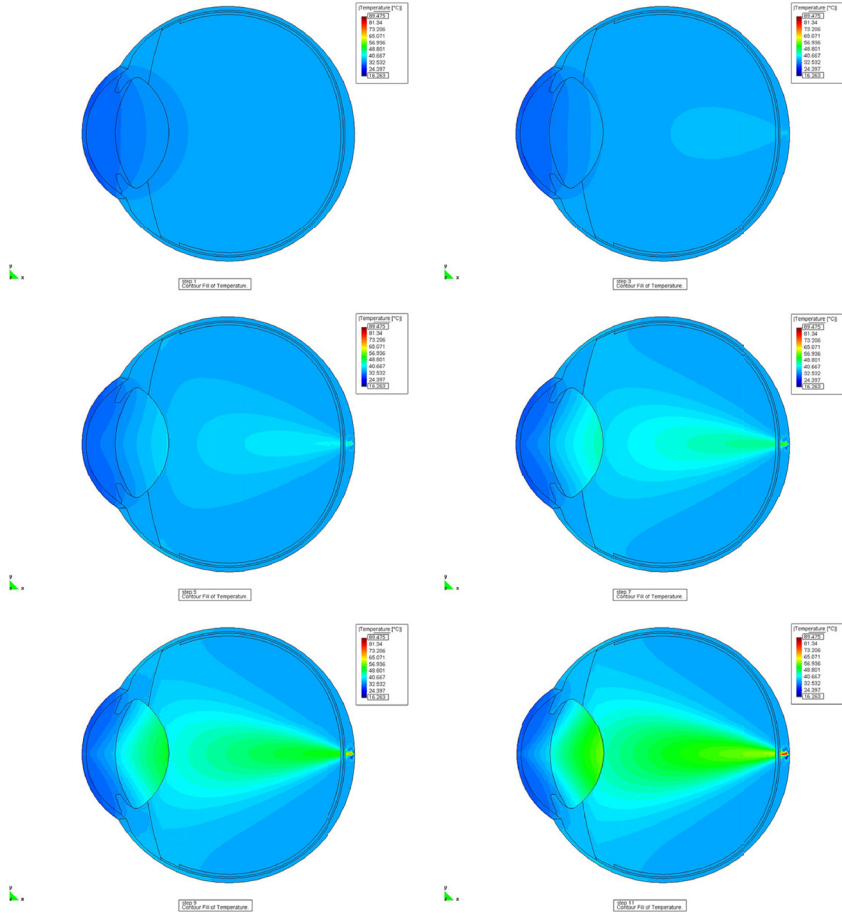


Figure 5: Evolution of temperature distribution in the whole eye, after $t = 0$ ms, 0.2 ms, 0.4 ms, 0.6 ms, 0.8 ms and 1 ms, achieved with 1064 nm Nd:YAG laser.

wavelengths, as seen from Figure 2, since lens thermal conductivity significantly less effects the temperature as seen from Tables 2 and 3.

4 Conclusion

Thermal model of the human eye exposed to infrared laser radiation has been developed to calculate the temperature distribution. The mathematical model is based on the space–time dependent Pennes’ bioheat transfer equation, taking into account different types of heat transfer processes. Calculation has been done for two infrared laser wavelengths, 1064 nm Nd:YAG and 2090 nm Ho:YAG, widely

Table 2: The effect of thermal conductivity of lens on the temperature distribution within the eye.

k_l (J/ms°C)	Node 3	Node 9	Node 169	Node 424	Node 1118
0.21	30.847	33.347	32.292	34.38	38.229
0.40	31.062	33.555	32.614	34.827	38.198
0.60	31.202	33.69	32.822	35.117	38.187

Table 3: The effect of thermal conductivity of lens on the temperature distribution within the eye.

k_l (J/ms°C)	Node 1985	Node 10421	Node 10537	Node 10782	Node 10913
0.21	41.946	40.244	38.403	43.163	58.478
0.40	41.516	40.227	38.387	43.149	58.466
0.60	41.256	40.217	38.377	43.141	58.459

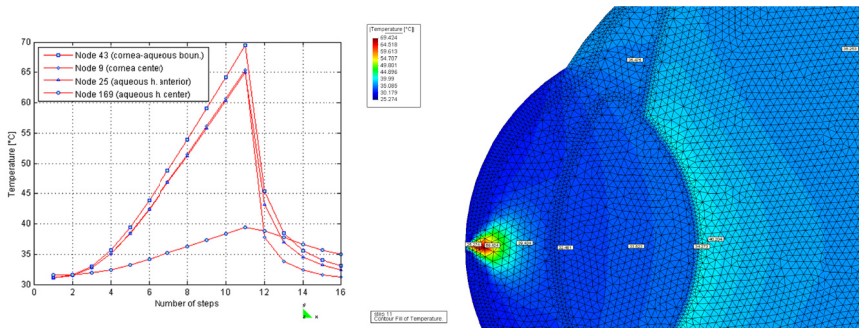


Figure 6: Detail of temperature distribution around anterior part of the eye and temperature evolution of nodes on corneo-aqueous boundary, cornea, aqueous and vitreous humour for 1 ms exposure and relaxation after source cancelling, achieved with 2090 nm Ho:YAG laser.

used in ophthalmology. Results show maximum temperatures of 89.475°C in posterior part of eye and 69.424°C in anterior part of eye, for Nd:YAG and Ho:YAG, respectively. Also, results for Ho:YAG laser show that lens functions as an optical filter for infrared radiation of this particular wavelength, due to high absorption coefficient value.

References

[1] Thompson, K., Ren, Q. & Parel, J., Therapeutic and diagnostic application of lasers in ophthalmology. *Proceedings of the IEEE*, **80(6)**, 1992.



- [2] Podol'tsev, A. & Zheltov, G., Photodestructive effect of IR laser radiation on the cornea. *Optics and Spectroscopy*, **102(1)**, pp. 142–146, 2007.
- [3] Taflove, A. & Brodwin, M., Computation of the electromagnetic fields and induced temperatures within a model of the microwave-irradiated human eye. *Microwave Theory and Techniques*, **23**, pp. 888–896, 1975.
- [4] Emery, A., Kramar, P., Guy, A. & Lin, J., Microwave induced temperature rises in rabbit eyes in cataract research. *Journal of Heat Transfer*, **97**, pp. 123–128, 1975.
- [5] Scott, J., A finite element model of heat transport in the human eye. *Physics in Medicine and Biology*, **33(2)**, pp. 227–241, 1988.
- [6] Scott, J., The computation of temperature rises in the human eye induced by infrared radiation. *Physics in Medicine and Biology*, **33(2)**, pp. 243–257, 1988.
- [7] Legendijk, J., A mathematical model to calculate temperature distributions in human and rabbit eyes during hyperthermic treatment. *Physics in Medicine and Biology*, **27(11)**, pp. 1301–1311, 1982.
- [8] Mainster, M.A., Ophthalmic applications of infrared lasers – thermal considerations. *Investigative Ophthalmology & Visual Science*, **18(4)**, pp. 414–420, 1979.
- [9] Amara, E., Numerical investigations on thermal effects of laser-ocular media interaction. *International Journal of Heat and Mass Transfer*, **38(13)**, pp. 2479–2488, 1995.
- [10] Sbirlea, G. & L'Huillier, J., A powerful finite element for analysis of argon laser iridectomy - influence of natural convection on the human eye. *Transactions on Biomedicine and Health*, **4**, pp. 67–79, 1997.
- [11] Chua, K.J., Ho, J.C., Chou, S.K. & Islam, M.R., On the study of the temperature distribution within a human eye subjected to a laser source. *International Communications in Heat and Mass Transfer*, **32**, pp. 1057–1065, 2005.
- [12] Dodig, H., *EM and Thermal Modelling of the Human Eye*. Master's thesis, Wessex Institute of Technology, 2004.
- [13] Peratta, A., Electromagnetic modelling of human eye exposed to Conductive Keratoplasty. *WIT Transactions in Biomedicine and Health*, **12(VII)**, pp. 223–229, 2007.
- [14] DeMarco, S.C., Lazzi, G., Liu, W., Weiland, J.D. & Humayun, M.S., Computed SAR and thermal elevation in a 0.25-mm 2-D model of the human eye and head in response to an implanted retinal stimulator – Part I: Models and methods. *IEEE Transactions on Antennas and Propagation*, **51(9)**, pp. 2274–2285, 2003.
- [15] Makous, W. & Gould, J., Effects of lasers on the human eye. *IBM Journal of Research and Development*, **12(3)**, pp. 257–271, 1968.
- [16] Krauss, J., Puliafito, C. & Steinert, R., Laser interactions with the cornea. *Survey of Ophthalmology*, **31(1)**, pp. 37–51, 1986.
- [17] Carroll, L. & Humphreys, T.R., Laser-tissue interactions. *Clinics in Dermatology*, **24**, pp. 2–7, 2006.



- [18] Cvetković, M., Analysis of the Temperature Distribution to the Human Eye Exposed to Laser Radiation, 2008. To be published.
- [19] Pennes, H.H., Analysis of tissue and arterial blood temperatures in the resting human forearm. 1948. *Journal of Applied Physiology*, **85(1)**, pp. 5–34, 1998.
- [20] Minkowycz, W.J., Sparrow, E.M. & Murthy, J.Y., *Handbook of Numerical Heat Transfer, Second Edition*. John Wiley & Sons, Inc., New York, p. 1024, 2006.
- [21] Ng, E. & Ooi, E., FEM simulation of the eye structure with bioheat analysis. *Computer Methods and Programs in Biomedicine*, **82**, pp. 268–276, 2006.
- [22] Ooi, E., Ang, W. & Ng, E., Bioheat transfer in the human eye: A boundary element approach. *Engineering Analysis with Boundary Elements*, **31(6)**, pp. 494–500, 2007.
- [23] Animated results. <http://marjan.fesb.hr/~mcvetkov/mfield/results2008/>.

